Relating target properties to the planimetric shape of simple impact craters

Wesley A. Watters[1] and Maria T. Zuber[2]; [1]Cornell University, Dept. of Astronomy, 610 Space Sciences Building, Ithaca, NY (watters@mit.edu); [2]MIT Dept. of Earth, Atmospheric and Planetary Sciences.

Overview

Our aim in this study is to illuminate the dependence of planimetric crater shape on the properties of geological targets, as well as modification state. We have measured the rim trace of 110 comparatively fresh impact craters in HiRISE images (i.e., craters with preserved ejecta), as well as 840 fresh craters in MOC images. From the planimetric shape (i.e., the rim trace) we compute a suite of morphometric quantities, including Fourier harmonic amplitudes and measures of the deviation from radial symmetry. We compare the distributions of these quantities for craters that formed in targets exhibiting a range of properties, noting all statistically meaningful differences. We have also measured the departure from radial symmetry of the planimetric shape as a function of crater diameter, in which a clear transition is noted between $D = 150$ and 250 m. Moreover, globally-distributed craters exhibit a strong lateral elongation bias that may reflect an independent measure of Mars' past obliquity variations.

Characterizing target properties

Target properties are characterized in two ways. First, we use context imagery to note salient features of surrounding terrain (outside of the ejecta) as well as some properties of the crater rim: e.g., (a) the presence or absence of aligned [systematic] joints, (b) the presence/absence of rocks and boulders that make up target materials, (c) presence/absence of significant mass movements on the upper rim wall. Second, we have used global digital geologic atlases ([1], [2], [3]) to query mapped units in which crater positions occur. All units have been assigned to the following material classes on the basis of mapped unit descriptions: (1) debris; (2) sedimentary; (3) debris + sedimentary; (4) lavas; (5) volcanics (lavas + debris); (6) mantled terrain (i.e., aeolian sediments and or lavas overlying older rocks). On the basis of these distinctions, the 110 craters in the HiRISE-FCC (HiRISE Fresh Crater Catalogue) and 840 in the MOC-FCC are divided into 13 subsets.

Morphometric quantities

We measure the crater diameter (D), planimetric diameter of cavity fill (or [flat] bottom diameter, L_F), and shadow length (S_0). From the shadow length and diameter (and solar incidence angle) we estimate the depth-diameter ratio (d_s/D), using the shape-dependent equations in [4], and in this way eliminate from consideration the few craters of probable secondary origin ($d_s/D < 0.12$). We also compute a "fill ratio" ($F \equiv L_F/D$), which is an informal estimate of the modification state of the crater, as well as the amount of sedimentary fill. As mentioned, we trace the rim crest and in this way obtain the planimetric shape of all impact craters in the catalogue. A circle is fit to this polygon to find the "deviation centroid": the point from which the standard deviation of radii is minimized. The rim trace is then resampled at 360 points, in polar coordinates with respect to the deviation centroid ($R(\theta_i)$ for $i = 1$ to 360). From this we compute numerous morphometric quantities including (but not limited to): (a) The standard radial deviation (i.e., standard deviation of radius, σ_R), as well as the same quantity normalized by mean radius: $\sigma_R^* \equiv \sigma_R/\bar{R}$; (b) the Fourier harmonic amplitudes and phase angles, defined implicitly by:

$$R(\theta_i) = A_0 + \sum_{n=1}^{360} A_n \cos(n\theta_i - n\phi_n) \qquad (1)$$

Results

We have compared the distributions of morphometric quantities for impact craters belonging to each of the 13 subsets mentioned above, and simple tests have been applied to find statistically meaningful differences (e.g., Kolmogorov-Smirnov). Several key results from these and other analyses are listed here:

a. Populations of craters forming in targets with clearly-expressed systematic joints as well as craters forming in non-lava targets have a larger fraction of squares (i.e., of craters whose largest harmonic amplitude is $n = 4$).

b. In Fig. 1 we have plotted the dependence of standard radial deviation (σ_R^*) upon crater diameter D in log-log space. A clear transition occurs at diameters in the range 150 m to 250 m, where radial deviation reaches a maximum (on average). This corresponds to diameters at which the transition from strength- to gravity-dominated excavation is expected to occur on Mars [5].

c. Above this diameter, the dependence is [approximately] a power-law decay. For subsets of the catalogue that exhibit the strongest correlation ($r = -0.8$) between radial deviation and diameter (e.g., craters formed in lavas and craters without evidence of major mass movements on their upper rim walls), the dependence is given

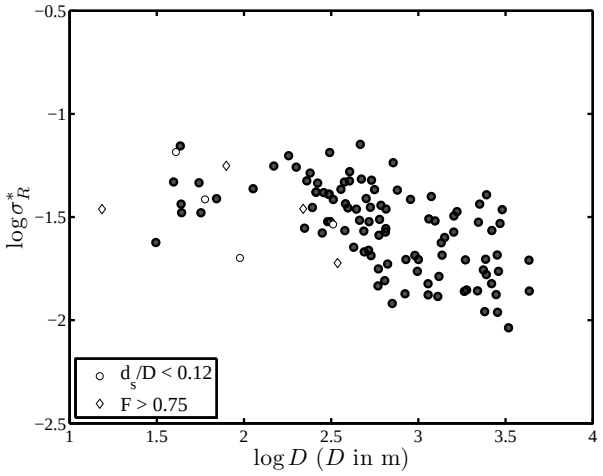

Figure 1: Standard radial deviation (σ_R^*) versus crater diameter D for 110 fresh craters in HiRISE images, where small depth-diameter ratio and large fill ratios are marked with open symbols. A significant transition occurs between D = 150 m and 250 m.

by:

$$\{\Delta R^*, \sigma_R^*\} \propto D^{-1/2} \tag{2}$$

By contrast, the subset with the weakest correlation ($r = 0.5$) correspond to craters formed in targets made up of unconsolidated or poorly-indurated debris. In this case, the dependence is far more gradual:

$$\{\Delta R^*, \sigma_R^*\} \propto D^{-1/4} \tag{3}$$

e. The major-axis elongation azimuth ϕ_E is the second harmonic phase angle ϕ_2 plus 90 degrees, mapped onto $[-90°, 90°]$. We have plotted the histogram of this angle (in degrees with respect to north) in Fig. 2 for 840 simple impact craters in MOC images. We find a strong lateral elongation bias in a globally-distributed population of impact craters: i.e., the planimetric shape of small craters tends to be elongated in a direction parallel to the equator. We have taken care to show this is not a consequence of illumination or resolution effects, and the global distribution of craters would seem to rule out modification alone. Recent work has shown that crater shape can reflect impact azimuth for even very slight incidence angles [6], suggesting that this approach may be used to supply an independent constraint on Mars' past obliquity variations (i.e., assuming all projectiles are sourced from the ecliptic plane).

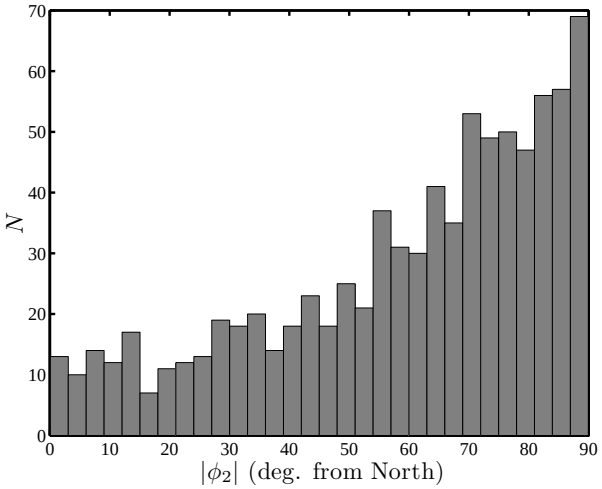

Figure 2: Absolute major axis elongation angle $|\phi_E|$ for 840 globally-distributed fresh craters in MOC images. This distribution indicates a strong lateral elongation bias: i.e., the tendency for small crater elongation to be parallel with the equator.

References

[1] R. Greeley and J.E. Guest. Geologic map of the eastern equatorial region of Mars, scale 1:15,000,000. *U.S. Geol. Survey Map*, I-1802-B, 1987.

[2] D. H. Scott and K. L. Tanaka. Geological map of the western equatorial region of Mars, scale 1:15,000,000. *U.S. Geol. Survey Map*, I-1802-A, 1986.

[3] K.L. Tanaka, Jr. J. A. Skinner, and T. M. Hare. Geologic map of the northern plains of Mars. *U. S. Geol. Survey Map*, SIM-2888, 2005.

[4] J.E. Chappelow and V.L. Sharpton. An improved shadow measurement technique for constraining the morphometry of simple impact craters. *Meteoritics and Planetary Science*, 37:479–486, 2002.

[5] M. J. Melosh. *Impact Cratering: A Geological Process*. Oxford Univ. Press, New York, 1st edition, 1989.

[6] D. Wallis, M.J. Burchell, A.C. Cook, C.J. Solomon, and N. McBride. Azimuthal impact directions from oblique impact crater morphology. *Monthly Notices of the Royal Astronomical Society*, 359:1137–1149, 2005.